

# An Evaluation of Haptic Cues on the Tele-Operator's Perceptual Awareness of Multiple UAVs' Environments

Hyoungh Il Son<sup>1\*</sup> Junsuk Kim<sup>2†</sup> Lewis Chuang<sup>1‡</sup> Antonio Franchi<sup>1§</sup> Paolo Robuffo Giordano<sup>1¶</sup>  
Dongjun Lee<sup>3||</sup> Heinrich H. Bühlhoff<sup>1,2\*\*</sup>

<sup>1</sup>Department of Human Perception, Cognition and Action, Max Planck Institute for Biological Cybernetics

<sup>2</sup>Department of Brain and Cognitive Engineering, Korea University

<sup>3</sup>Department of Mechanical, Aerospace and Biomedical Engineering, University of Tennessee at Knoxville

## ABSTRACT

The use of multiple unmanned aerial vehicles (UAVs) is increasingly being incorporated into a wide range of teleoperation applications. To date, relevant research has largely been focused on the development of appropriate control schemes. In this paper, we extend previous research by investigating how control performance could be improved by providing the teleoperator with haptic feedback cues. First, we describe a control scheme that allows a teleoperator to manipulate the flight of multiple UAVs in a remote environment. Next, we present three designs of haptic cue feedback that could increase the teleoperator's environmental awareness of such a remote environment. These cues are based on the UAVs' i) velocity information, ii) proximity to obstacles, and iii) a combination of these two sources of information. Finally, we present an experimental evaluation of these haptic cue designs. Our evaluation is based on the teleoperator's perceptual sensitivity to the physical environment inhabited by the multiple UAVs. We conclude that a teleoperator's perceptual sensitivity is best served by haptic feedback cues that are based on the velocity information of multiple UAVs.

**Index Terms:** H.5.2 [Information Interfaces and Presentation]: User Interfaces—Evaluation/methodology, Haptic I/O

## 1 INTRODUCTION

The past decade has seen significant improvements to the operation of unmanned aerial vehicles (UAVs) via a master-slave system (see [1] for a recent overview). In addition, teleoperation systems of multiple UAVs have more recently emerged to compensate for the limitations of traditional single-master-single-slave configurations. For example, a teleoperation system of multiple slaves allows multiple tasks to be completed within a shorter time and increases the area coverage at a lower cost. Current research on this theme is mostly focused on developing different bilateral teleoperation algorithms to control multiple slaves more efficiently and robustly (see [2, 3, 4] for more details). In contrast, considerably less attention has been devoted towards understanding how the performance of teleoperators can be improved with such systems (however, see [5, 6, 7] for conventional teleoperation)

\*e-mail: hyoungil.son@tuebingen.mpg.de

†e-mail: wowkjs@korea.ac.kr

‡e-mail: lewis.chuang@tuebingen.mpg.de

§e-mail: antonio.franchi@tuebingen.mpg.de

¶e-mail: paolo.robuffo-giordano@tuebingen.mpg.de

||e-mail: djlee@utk.edu

\*\*e-mail: heinrich.buehlhoff@tuebingen.mpg.de

In a previous paper [3], we proposed a passive teleoperation control strategy that allows a stable topology of multiple UAVs to be maintained, by using repulsive and attractive forces between UAVs. Besides this, additional repulsive forces were introduced between the UAVs and their physical environment to improve obstacle avoidance on the part of the teleoperator. These repulsive and the attractive forces were designed as functions that took into account the relative distances between UAVs as well as the UAV and obstacle(s). In our control scheme, the human operator provides a velocity command to remote UAVs via the position of a haptic device controller that is situated at his workstation, in order to indefinitely extend the workspace of UAVs. Moreover, the forces experienced by this multiple UAV scheme can be transmitted back to the operator in the form of haptic cues, such as to facilitate the operator's control performance. In this paper, we further this previous work by discussing how such forces can be appropriately transformed into haptic cues before presenting a systematic evaluation of the contribution of these cues to teleoperation performance.

One of common control objectives in conventional bilateral teleoperation is to ensure that the force of the master, which is handled by a human operator, effectively tracks the force of the remote slave as it interacts with its immediate environment [8]. Good force tracking is expected to bring about better perceptual awareness on the part of the teleoperator, of the remote environment that the controlled slave inhabits. This is important given that known limitations of on-board cameras (e.g., restricted field of view (FOV), poor camera resolution) [9] can significantly restrict the availability of visual information necessary for effective UAV control. To elaborate, perceptual awareness is especially important to avoid collisions between the controlled vehicles and environmental obstacles. Thus, force tracking can be a useful measure for evaluating the performance of a control scheme for conventional bilateral teleoperation.

Unfortunately, this does not directly apply to the control of multiple UAVs. This is because there is typically no direct physical contact between UAVs and their environments, at least none that would be desirable. Hence, it is not clear which forces ought to be transmitted to the operator for achieving effective force tracking; in a way that would be comparable to established conventional teleoperation studies in free motion and contact motion (e.g., [10]). Nevertheless, we can fabricate haptic feedback schemes in the teleoperation of multiple UAVs, that could serve the purpose of increasing the operator's perceptual awareness of the UAVs' remote environment. The proposed schemes in this paper are explained in detail in Section 3.

In spite of this, it remains that force tracking may not be a measurable concept that can be directly generalized to teleoperation systems for UAVs. Achieving good force tracking with a fabricated interaction force between the UAVs and their environments may not guarantee better perceptual awareness of the remote environment, on the part of the operator. With this in mind, we decided

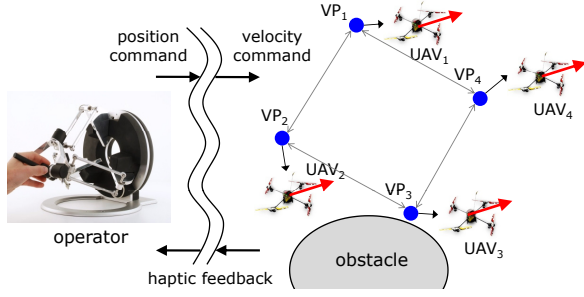


Figure 1: Haptic teleoperation of multiple UAVs.

to assess the performance of our multiple UAV teleoperation systems by directly measuring the perceptual sensitivity of the human operator. The basic concept of an experimental design for the evaluation of the operator's perceptual awareness of multiple UAVs' environments was presented by the authors in [11]. Performance of the proposed teleoperation system in [3] depends heavily on the repulsive and attractive force functions between the UAVs and their obstacle environments, the haptic feedback cue which is transmitted to the human operator and a teleoperation control which is used to transmit the desired haptic cue. Here, we measured the influence of various haptic feedback algorithms (i.e., the combination of the haptic cue and the teleoperation control) on teleoperation performance, based on the bilateral teleoperation control architecture proposed in our previous study [3].

The structure of this paper is as follows. First, we review our framework for haptic teleoperation of multiple UAVs. Following this, we describe possible designs of haptic feedback cues that could serve to increase perception of the remote environment of controlled UAVs. Finally, we provide a psychophysical evaluation of these haptic feedback cues and teleoperation controls to determine the cue and the control that achieves the best level of environment perception.

## 2 BILATERAL TELEOPERATION OF MULTIPLE UAVS

In our previous research [3], we proposed a novel semi-autonomous haptic teleoperation framework for multiple quadrotor-type UAVs. This enables a single human user to stably teleoperate multiple remote UAVs over the Internet with varying-delay/packet-loss. It also provides useful haptic feedback cues to the teleoperator, designed to increase perceptual awareness as well as control performance. Hereafter, we briefly review these layers and refer the reader to [3] for further details.

Our framework consists of the following three control layers (see Fig. 1):

1. **UAV control layer**, that each UAV to track the trajectory of its own kinematic Cartesian virtual point (VP). For this, we assume availability of some reasonably-good trajectory tracking control laws (e.g., [12]) for the UAVs, which then allow us to abstract the UAVs by their kinematic VPs, while bypassing the issues of the UAVs' low-level control;
2. **VP control layer**, that modulates the motion of VPs in such a way that, as a whole, they behave as a deformable (multi-node) flying object, whose shape is autonomously adjusted according to local artificial potentials (designed for inter-VP/VP-obstacle collision avoidance and inter-VP connectivity preservation), the bulky motion of which is driven by teleoperation velocity commands received from the master side;
3. **teleoperation layer**, that enables the human user to teleoperate this VPs network, while haptically perceiving the state

of the real UAVs over the Internet. For this, passive set-position modulation (PSPM [13]) is adopted for its flexibility (e.g., to address master-slave kinematic dissimilarity due to the fact that the master workspace bounded while the UAVs workspace is unbounded), guarantee of passivity, and less conservative passifying action (thus yielding better performance).

We consider  $N$  quadrotor-type unmanned aerial vehicles (UAVs), each with underactuated Lagrangian dynamics in  $SE(3)$  [12]. The Cartesian position of each UAV is represented as  $x_i \in \mathfrak{R}^3$  is w.r.t. the NED (north-east-down) inertial frame. The quadrotors are endowed with an attitude controller which is able to track a desired trajectory in  $\mathfrak{R}^3$ , specified by the VP control layer.

On the other hand, we consider a 3-degree-of-freedom (DOF) haptic device as modeled by

$$M(q)\ddot{q} + C(q, \dot{q})\dot{q} = \tau + f \quad (1)$$

where  $q \in \mathfrak{R}^3$  is the configuration,  $M(q) \in \mathfrak{R}^{3 \times 3}$  is the positive-definite/symmetric inertia matrix,  $C(q, \dot{q}) \in \mathfrak{R}^{3 \times 3}$  is the Coriolis matrix, and  $\tau, f \in \mathfrak{R}^3$  are the control and human forces, respectively.

To teleoperate the 3-DOF Cartesian position of  $N$  UAVs, we endow each UAV with a 3-DOF Cartesian VP,  $p_i \in \mathfrak{R}^3$ . The human user will then teleoperate some (or all) of these  $N$  VPs over the Internet, while the real UAV's position,  $x_i$ , is tracking the trajectory of its own VP,  $p_i$ .

We implement the following kinematic evolution of VP on each UAV: for the  $i^{\text{th}}$  UAV,

$$\dot{p}_i(t) := u_i^t + u_i^c + u_i^o \quad (2)$$

where

1.  $u_i^c \in \mathfrak{R}^3$  embeds the inter-VP collision avoidance and connectivity preservation, as defined by

$$u_i^c := - \sum_{j \in \mathcal{N}_i} \frac{\partial \varphi_{ij}^c (\|p_i - p_j\|^2)^T}{\partial p_i} \quad (3)$$

where  $\varphi_{ij}^c$  is a certain artificial potential function to create attractive action if  $\|p_i - p_j\|$  is large, and repulsive action if  $\|p_i - p_j\|$  small, and

$$\mathcal{N}_i := \{j \mid (j, i) \in \mathcal{E}(G)\}$$

i.e. connectivity neighbors of the  $i^{\text{th}}$  VP;

2.  $u_i^o \in \mathfrak{R}^3$  is the obstacle avoidance control given by

$$u_i^o := - \sum_{r \in \mathcal{O}_i} \frac{\partial \varphi_{ir}^o (\|p_i - p_r^o\|)^T}{\partial p_i} \quad (4)$$

where  $\mathcal{O}_i$  is the set of the obstacles of the  $i$ -th VP with  $p_r^o$  being the position of the  $r^{\text{th}}$  obstacle in  $\mathcal{O}_i$ , and  $\varphi_{ir}^o$  is a certain obstacle avoidance artificial potential, which produces repulsive action if  $\|p_i - p_r^o\|$  is small and vanishes as  $\|p_i - p_r^o\| \rightarrow \infty$ ;

3.  $u_i^t \in \mathfrak{R}^3$  will contain the teleoperation control for a (non empty) subset  $\mathcal{N}_i \subset \{1, 2, \dots, N\}$  among the  $N$  VPs, to enable a remote human user to tele-drive the Cartesian velocity of the  $N$  VPs network over the Internet.

To begin, in the teleoperation layer that enables a remote human user to tele-control the VPs/UAVs, we define  $u_i^t$  in (2) s.t., for  $t \in [t_k^s, t_{k+1}^s)$ ,

$$u_i^t(t) := \lambda q(k), \quad \forall i \in \mathcal{N}_l \quad (5)$$

where  $q(k)$  is the master position  $q(t) \in \mathfrak{R}^3$  received via the Internet at the (slave) reception time  $t_k^s$ , and  $\lambda > 0$  is to match different scales between  $q(t)$  and  $\hat{p}_i$ . This control (5) enables the user to tele-control the VPs' velocities  $\hat{p}_i$  via the master device position  $q(t)$ , thereby, allowing us to circumvent master-slave kinematic/dynamic dissimilarity.

On the other hand, to enable the user to tele-sense all the VPs/UAVs collectively, we can design the haptic feedback signal  $y(t) \in \mathfrak{R}^3$  to be sent to the master, s.t.

$$f : (\dot{x}_i, u_i^o) \mapsto y(t) \quad (6)$$

where  $\dot{x}_i$  is the UAV's velocity, and  $u_i^o$  is the VP's obstacle avoidance control (4).

This  $y(t)$  is then sent to the master over the Internet. Let us denote by  $y(k)$  its reception by the master side over the Internet at the (master) reception time  $t_k$ . We incorporate this  $y(k)$  into the teleoperation control  $\tau$  in (1) s.t.

$$f : (q, \dot{q}, \bar{y}(k)) \mapsto \tau(t) \quad (7)$$

for  $t \in [t_k, t_{k+1})$ , where  $\bar{y}(k)$  is the PSPM-modulation of  $y(k)$ .

In this study,  $y(t)$  and  $\tau(t)$  in (6) and (7), are respectively treated as the design of the haptic cue and the teleoperation control.

### 3 HAPTIC FEEDBACK ALGORITHM DESIGN

In conventional teleoperation systems, there are three classes of haptic cues that can serve as feedback to the operator site from the remote UAVs; namely, the position of the slave, the force of the slave, and a combination of the position and the force of the slave [10].

Generally, a control input to the haptic device can be designed as

$$\tau = -C_p(q - x) - K_f f \quad (8)$$

where  $x \in \mathfrak{R}^3$  and  $f \in \mathfrak{R}^3$  are, respectively, the position and the force of the slave, and  $C_p$  and  $K_f$  denote a position controller and a force controller respectively [10].

From this, three cases of control schemes are conceivable. A position error-based control (or position-position control, hereafter referred to as PP control), a direct force feedback control (or force-position control, hereafter referred to as FP control), and a three channel control (hereafter referred to as PFP control). Respectively, they fulfil the conditions of ' $C_p = K + Bs$  and  $K_f = 0$ ' (for the PP) where  $B, K, K_f \in \mathfrak{R}^{3 \times 3} \succ 0$  are diagonal gain matrices, ' $C_p = 0$  and  $K_f \neq 0$  (usually, selected as one)' (for the FP), and ' $C_p = K + Bs$  and  $K_f \neq 0$ ' (for the PFP).

With this in mind, we selected three kinds of haptic cues based on the PP, FP, and PFP controls to design  $y(t)$  in (6), which influences the teleoperation control  $\tau$  in (7) accordingly. In addition, control parameters are selected as  $K, B$ , and  $K_f$  for each haptic cue. Details for the design of haptic cues and control parameters are presented in the following sub-sections.

#### 3.1 Haptic Cues

For the teleoperation of multi-UAVs, information from the remote UAVs (or  $y(t)$  in (6)) are designed as:

- Case 1: velocity information of UAVs,

$$y(t) = \frac{1}{\lambda N} \sum \dot{x}_i \quad (9)$$

- Case 2: obstacle avoidance force,

$$y(t) = \frac{1}{\lambda N} \sum u_i^o \quad (10)$$

- Case 3: both velocity information of UAVs and obstacle avoidance force,

$$y(t) = \frac{1}{\lambda N} \sum (\dot{x}_i + u_i^o) \quad (11)$$

according to PP control, FP control, and PFP control, respectively.

#### 3.2 Teleoperation Control

It follows that  $\tau(t)$  in (7) can be respectively designed for these three types of haptic cues as:

- For case 1 of  $y(t)$ :

$$\tau(t) = -B\dot{q} - K[q - \bar{y}(k)] \quad (12)$$

- For case 2 of  $y(t)$ :

$$\tau(t) = -B\dot{q} - K\bar{y}(k) \quad (13)$$

- For case 3 of  $y(t)$ :

$$\tau(t) = -B\dot{q} - K[q - \bar{y}(k)]. \quad (14)$$

Hereafter, cases 1, 2, and 3 of the haptic cue and the teleoperation control will be referred to as *Velocity*, *Force*, and *Velocity+Force*.

The *Velocity* cue allows the human operator to directly perceive the 'inertia' of the UAVs using (9). It should also indirectly indicate the presence of obstacles because obstacles that obstruct the UAV motion will induce an increase in the tracking error between  $\hat{p}_i$  and  $\dot{x}_i$ . Therefore, maneuvering the UAVs toward the obstacles should transmit a strong haptic feedback to the teleoperator. With the *Force* algorithm, a force is fed back to the human only when an obstacle is detected. From this, it follows that the *Velocity+Force* cue is equivalent to the *Velocity* cue, in the absence of obstacles. However, the *Velocity+Force* cue should result in a larger haptic force feedback than the separate cues of *Velocity* and *Force* when obstacles are present.

It should be noted that  $\tau(t)$  is not designed as  $-B[\dot{q} - \dot{\bar{y}}(k)] - K[q - \bar{y}(k)]$ , which is the same scheme as the PP control for the  $\tau(t)$  of the first case, because it cannot be guaranteed the system passivity with the PSPM. In the  $\tau(t)$  of *Velocity+Force*,  $\tau(t)$  is not designed as  $-B[\dot{q} - \dot{\bar{y}}_1(k)] - K[q - \bar{y}_1(k)] - K_f \bar{y}_2(k)$  where  $y(t) = y_1(t) + y_2(t) = \frac{1}{\lambda N} \sum \dot{x}_i + \frac{1}{\lambda N} \sum u_i^o$  because the PSPM cannot modulate and transmit information separately. Due to these limitations of the PSPM we can expect a decrease of the operator's performance when (12) and (14) are used, especially at transient states of UAVs. We will try to overcome the limitations by modifying the PSPM in a follow-up study.

Our *Force* cue differs from the conventional FP control, with the inclusion of a damping term in (13). This allows a level of stability robustness to be maintained, equivalent to *Velocity* and *Velocity+Force*. Although, this additional term could decrease overall performance due to known tradeoffs between the performance and stability in teleoperation systems, it was included to allow for fair comparisons between the three cues.

The design of  $u_i^o$  is also expected to influence the performance of (10) and (11). For simplicity, we use  $u_i^o$  designed in (4). Future work could address how  $u_i^o$  could be designed for better performance.

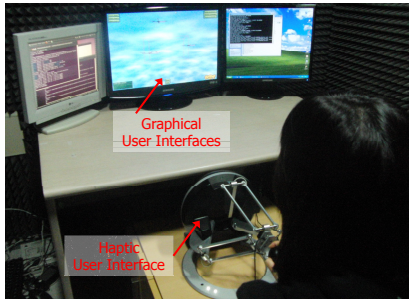


Figure 2: Experimental setup. Graphical User Interfaces (GUIs) and Haptic User Interface (Omega Device).

### 3.3 Control Parameters

The teleoperation control  $\tau(t)$  is varied for the parameters  $K$  and  $B$  for each haptic cue. The following guidelines have been proposed for the selection of control parameters in PSPM: 1) select  $K$  to be as large as possible under stable behavior for sharp perception/tracking; 2) select  $B$  to be as small as possible under stable behavior for motion agility. These control parameters are expected to provide a tradeoff between performance and stability [13] and the functional relationship(s) between these control parameters and performance stability and operator performance constitute ongoing research. In the current work, these control parameters are fixed across the haptic cues.

## 4 PSYCHOPHYSICAL EVALUATION OF HAPTIC CUE FEEDBACK ON TELEOPERATION

The previous section presented three types of haptic cue feedback that could improve teleoperation performance (see Section 3). Such cues are designed to communicate the remote environment of the controlled UAVs to the teleoperator. In this section, we report a psychophysical experiment that directly evaluated each respective cue for its ability to do so. Here, participants were required to discriminate between two adjacent walls that differed in varying levels of distance from the UAVs. They did so by probing them with a UAV swarm. We consider the ideal haptic cue to be the one that resulted in the most sensitive discrimination performance.

### 4.1 Participants

Eighteen students (14 males; age range: 20-33 years) of Korea University, Seoul participated in this experiment and were paid approximately \$13 USD for their time. All participants were naive to the experiment and apparatus. They possessed normal or corrected-to-normal eyesight and possessed no physical disability. The experiment was conducted in accordance with the requirement of the Helsinki Declaration.

### 4.2 Apparatus

A haptic device for controlling a swarm of four UAVs and a virtual environment for the UAVs comprised the setup for our experiment.

Commercial haptic devices (Omega 3, Force Dimension) provided participants with the ability to control the UAVs in the experiment. The Omega 3 is a 3-DOFs haptic device with 3 translational actuated axes and its local control loop runs at about 2.5 kHz on a dedicated linux machine.

The dynamics and control logic of the UAVs were simulated in a custom-made simulation environment. This environment was based on the Ogre3D engine (for 3D rendering and computational geometry computations), and on the PhysX libraries for simulating the physical interaction between the UAVs and the environment. The simulation runs at 60 Hz and dictates the data exchange rate between the haptic device and virtual UAVs. An experimental setup is

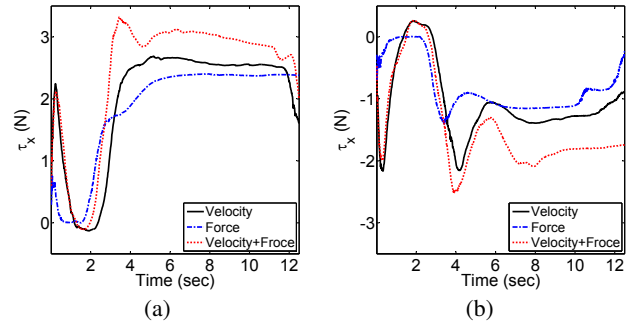


Figure 3: Force profile with (a) Right-side obstacle. (b) Left-side obstacle. The forces were measured when UAVs were maneuvered toward the right-side or left side obstacle from a same position and then maintained their position over 5 seconds by the operator.

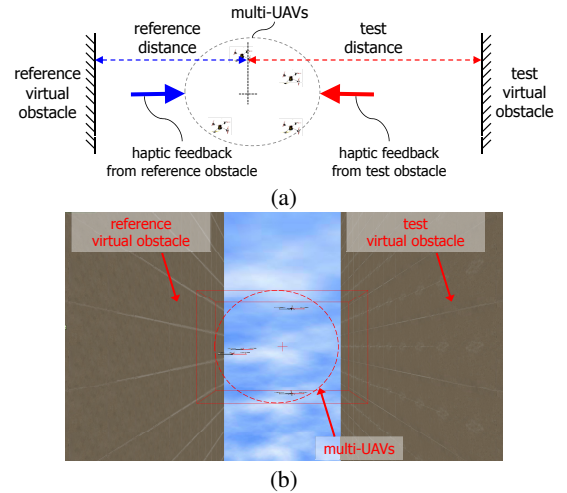


Figure 4: Test of environment perception. (a) Experimental design. (b) Screen shot of the perception test.

shown in Fig. 2. The simulated UAVs and environment is presented in the center monitor. An instruction about a manipulation of the omega is shown in the first (left) monitor which is connected with the linux machine. The right monitor shows informations about the experiment procedure.

In this virtual environment, the UAV swarm constantly assumed a tetrahedron formation, with an inter-UAV distance of approximately 0.8 m. They are always hovering between two walls of varying distance and their horizontal movements could be controlled by the haptic device. This visual scene is rendered from a camera perspective that was 8 m away from the starting positions of the UAVs, with the FOV of about  $21^\circ$ .

### 4.3 Procedure

There are several psychophysical methods to find the relation between stimulus and sensation. We used the method of constant stimuli [14] for determining the sensory thresholds of our participants in the current experiment.

The experiment was divided into three blocks of trials, for the three different types of haptic cues; namely, *Velocity*, *Force*, and *Velocity+Force*. The following control parameters (gains) were fixed for the purpose of this experiment:  $K=70\text{N/m}$  and  $B=2\text{Ns/m}$  for all haptic cues. This way, the produced force of the *Velocity* cue was comparable with the force of the *Force* cue, and less than the one generated by the *Velocity+Force* cue algorithm (see Fig. 3). Also,

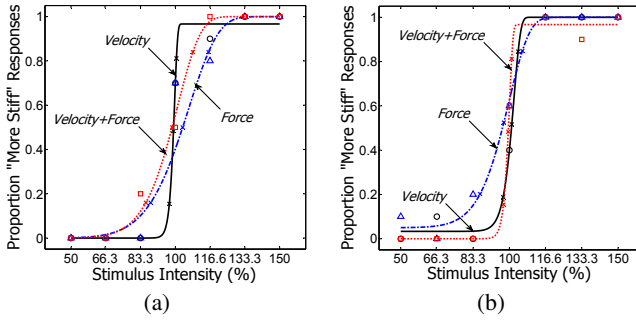


Figure 5: Discrimination sensitivity profile for three different types of haptic cues, for (a)Participant 1., (b)Participant 9. Steeper slopes indicate that the participant was better able to discriminate between smaller differences of obstacle stiffness.

the presentation order of the blocks was counter-balanced across the participants, such as to minimize the influence of practice on our findings.

The task was the same on every trial, regardless of the haptic cue type. On each trial, participants were presented with a swarm of four UAVs that were located between two obstacles (see Fig. 4). Their task was to determine which of the two obstacles was stiffer and they were expected to do this by controlling the UAVs to probe the obstacles. The UAV swarm was controlled by operating the haptic device, which also provided the condition-appropriate haptic cue. After probing the obstacles, participants indicated the stiffer of the two obstacles by using a mouse to click on one of two possible buttons that were located at the left or right position of the screen, which corresponded to the respective positions of the obstacles.

It is important to note that only the UAVs were visible to the observer. We rendered the obstacles invisible, so as to minimize any possible influence of visual feedback on their discrimination responses [15]. This allowed us to more accurately assess the influence of our haptic cue feedback.

Throughout the experiment, one obstacle was held at a constant stimulus level (distance, 3.4m) while the other differed from this reference wall across 7 levels of relative stimuli, from 50% to 150% in equal steps. The positions of the obstacles, relative to each other, were counterbalanced throughout the experiment and there were 10 trials for each level of tested difference, resulting in a total of 70 trials per block. These trials were completely randomized for presentation order.

The subjects were given a detailed tutorial about the experiment and were provided a training session with the Omega about 10 minutes to get them familiarized with the haptic device and the procedure. It took about 20 seconds for each trials. Ten minute breaks were provided between the blocks of trials and the entire experiment took 90 minutes to perform.

#### 4.4 Results

Psychometric functions were fitted to the collected data to assess each participant for their discrimination sensitivity, given a particular haptic cue. They were derived using the psignifit toolbox for Matlab which implements the maximum-likelihood method described in [16]. Examples are shown for two participants in Fig. 5. These plots denote the cumulative probability that the test obstacle would be perceived to be stiffer than the reference obstacle, as a function of its relative stiffness. Therefore, a steeper slope would correspond to discrimination performance that was more sensitive.

Discrimination sensitivity was measured as the difference of stiffness values between the 16th and 84th percentile. This value can be referred to as the just-noticeable difference (JND) [14] and denotes the difference in stimulus intensity that participants were

Table 1: A summary of the JNDs of all participants for the different haptic cue conditions.

Subject	Haptic Cue			Best	Worst
	Velocity	Force	Vel.+For.		
S1	3.42	27.72	22.53	Velocity	Force
S2	24.80	30.68	17.80	Vel.+For.	Force
S3	6.88	25.49	25.80	Velocity	Vel.+For.
S4	25.74	27.29	17.87	Vel.+For.	Force
S5	5.44	28.48	5.04	Vel.+For.	Force
S6	35.47	57.63	24.42	Vel.+For.	Force
S7	17.59	17.59	28.81	Vel., For.	Vel.+For.
S8	17.59	22.55	21.02	Velocity	Force
S9	6.92	19.48	3.80	Vel.+For.	Force
S10	28.72	44.35	46.08	Velocity	Force
S11	7.59	45.41	49.69	Velocity	Vel.+For.
S12	5.80	30.62	31.41	Velocity	Vel.+For.
S13	6.41	6.88	25.80	Velocity	Vel.+For.
S14	6.88	25.80	25.15	Velocity	Force
S15	5.51	23.08	18.03	Velocity	Force
S16	21.68	27.05	22.34	Velocity	Force
S17	25.49	35.24	5.25	Vel.+For.	Force
S18	6.88	17.59	31.56	Velocity	Vel.+For.
Mean	14.38	28.50	23.47		
Std. Error	2.41	2.75	2.88		

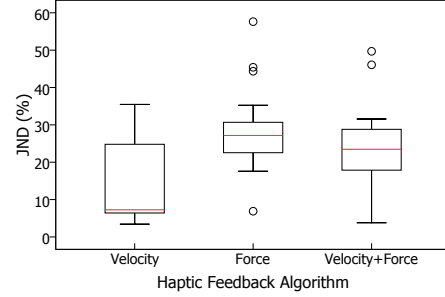


Figure 6: Summary of JNDs across the haptic cue conditions. Medians are indicated in red, boxes denote the interquartile range. The whiskers denote the range of data except outliers which are pre-represented as  $\circ$ .

able to reliably detect over one standard deviation around the point of subject equality<sup>1</sup> (PSE). A smaller value indicates greater sensitivity in discrimination; that is, better environmental awareness. The JNDs of all the participants across the experimental condition are summarized by Table 1 and Fig. 6.

From Table 1, it can be seen that the haptic cue of *Velocity* produced smaller JNDs compared to haptic cues *Force* ( $28.50 \pm 11.66$ ) and *Velocity+Force* ( $23.47 \pm 12.20$ ), respectively. In other words, participants were more sensitive to their environment when the *Velocity* cue was available, compared to when the obstacle avoidance force cue was provided instead. This finding is supported by a formal statistical test, which is reported in the following paragraph. The tested behaviour of participant 1 is typical of most of the participants and his derived psychometric functions for the three classes of cues are shown in Fig. 5(a). It can be observed from his plotted performance that the availability of the *Velocity* cue allowed him to reliably discriminate between smaller differences in stiffness compared to when only the *Force* cue was provided or a combination of the *Velocity+Force* cue.

Most participants were least sensitive in their discrimination responses with the *Force* cue, although some participants (i.e., S3,

<sup>1</sup>this is value of relative stiffness for which the test obstacle is perceived to be equally stiff to the reference obstacle

S7, S11, S12, S13, and S18) were least sensitive with the *Velocity+Force* cue. However, it is also interesting to note that other participants demonstrated greatest sensitivity for the *Velocity+Force* cue; namely, Participants 2, 4, 5, 6, 9, and 17 (see Fig. 5(b)).

We conducted a repeated measures analysis of variance (ANOVA) to formally determine if there were statistically significant differences between the performance measures across these three types of haptic cues. The results indicate that there was a significant main effect across the experimental condition of haptic cue type ( $F(2,34)=10.0$ ,  $p<0.001$ ). Post-hoc comparisons corroborated our earlier inference that the *Velocity* cue induced more sensitive performance than the *Force* cue ( $t(1,17)=5.84$ ,  $p<0.017^2$ ). All other post-hoc comparisons were statistically non-significant<sup>3,4</sup>.

Finally, the mean PSEs for the three haptic cue conditions were 99.7 (*Velocity*), 99.0 (*Force*), 101.1 (*Velocity+Force*). One sample t-tests confirmed that these PSEs were not different from 100% intensity level of the reference wall's physical stiffness. They were also not significantly different across the three conditions of haptic cue types ( $F(2,34)=2.18$ ,  $p=0.13$ ). This assured us of the validity of our evaluation and that our haptic cues were not likely to have introduced any systematic bias in responding.

## 5 SUMMARY AND CONCLUSIONS

In this study, we have presented a framework that allows haptic cues to be transmitted from the controlled UAVs to the teleoperator's controller. These cues can be designed to increase the teleoperator's perception on the remote environment that the UAVs inhabit and for this purpose, we proposed three possible types of haptic cues which are based on conventional teleoperation control.

The findings of our psychophysical evaluation indicate that a cue which is based on the velocity information of the UAVs is most likely to result in better environmental sensitivity while a cue based on the obstacle avoidance force results in relatively worse sensitivity. Interestingly, this result contradicts conventional knowledge in teleoperation control. Previous work have argued that cues that provide force information on sensed remote environments tend to support better perceptual awareness [7, 10]. The utility of the *Velocity+Force* cue varies for individual participants and can induce both the best as well as the worst performance (see Table 1). This could be because the additional *Force* cue could be perceived as being either an additional source of information or a confounding cue by our participants.

Overall, the current findings suggest that the perceptual awareness of human operator on remote environments is best served by a haptic feedback that is based on the velocity information of the UAVs. This approach of evaluating fabricated haptic cues for their influence on performance should allow us to design better algorithms for controlling multiple UAVs. In addition, our findings should be applicable to the teleoperation of a single robot (e.g. [9] for a mobile robot and [17] for a UAV).

It is worth mentioning that the utility of different cues is expected to vary according to the task of the teleoperator. In a parallel study, we have found that the *Force* cue induces better multi-UAV maneuverability by reducing control effort, relative to the *Velocity* cue [18]. Hence, there exists a clear challenge in establishing the appropriate employment of haptic cues according to the changing demands of multi-UAV control.

## ACKNOWLEDGEMENTS

This research was supported by the Max Planck Society and WCU(World Class University) program through the National Research Foundation of Korea funded by the Ministry of Education, Science and Technology (R31-10008).

<sup>2</sup>Bonferroni corrected for 3 post-hoc comparisons, alpha-level is 0.017

<sup>3</sup>*Velocity* vs. *Velocity+Force*:  $t(1,17)=2.44$ ,  $p=0.026$

<sup>4</sup>*Force* vs. *Velocity+Force*:  $t(1,17)=1.51$ ,  $p=0.15$ .

## REFERENCES

- [1] K. P. Valavanis and K. P. Valavanis, *Advances in Unmanned Aerial Vehicles: State of the Art and the Road to Autonomy*. Springer Publishing Company, Incorporated, 2007.
- [2] E. Rodriguez-Seda, J. Troy, C. Erignac, P. Murray, D. Stipanovic, and M. Spong, "Bilateral teleoperation of multiple mobile agents: Coordinated motion and collision avoidance," *IEEE Transactions on Control Systems Technology*, vol. 18, no. 4, pp. 984–992, 2010.
- [3] D. Lee, A. Franchi, P. Robuffo Giordano, H. I. Son, and H. H. Bühlhoff, "Semi-autonomous haptic teleoperation of multiple unmanned aerial vehicles over the internet," in *IEEE International Conference on Robotics and Automation*, May 2011, to be presented.
- [4] A. Franchi, P. Robuffo Giordano, C. Secchi, H. I. Son, and H. H. Bühlhoff, "A passivity-based decentralized approach for the bilateral teleoperation of a group of UAVs with switching topology," in *IEEE International Conference on Robotics and Automation*, May 2011, to be presented.
- [5] P. Malysz and S. Sirouspour, "Nonlinear and filtered force/position mappings in bilateral teleoperation with application to enhanced stiffness discrimination," *IEEE Transactions on Robotics*, vol. 25, no. 5, pp. 1134–1149, 2009.
- [6] D. Botturi, M. Vicentini, M. Righele, and C. Secchi, "Perception-centric force scaling in bilateral teleoperation," *Mechatronics*, vol. 20, no. 7, pp. 802 – 811, 2010.
- [7] H. I. Son, T. Bhattacharjee, and H. Hashimoto, "Enhancement in operator's perception of soft tissues and its experimental validation for scaled teleoperation systems," *IEEE/ASME Transactions on Mechatronics*, p. 10.1109/TMECH.2010.2076826, 2010.
- [8] D. Lawrence, "Stability and transparency in bilateral teleoperation," *IEEE Transactions on Robotics and Automation*, vol. 9, no. 5, pp. 624–637, 1993.
- [9] N. Diolaiti and C. Melchiorri, "Teleoperation of a mobile robot through haptic feedback," in *Proceedings of IEEE International Workshop on Haptic Virtual Environments and Their Applications*, pp. 67–72, 2002.
- [10] K. Hashtrudi-Zaad and S. E. Salcudean, "Analysis of control architectures for teleoperation systems with impedance/admittance master and slave manipulators," *The International Journal of Robotics Research*, vol. 20, no. 6, pp. 419–445, 2001.
- [11] J. S. Kim, H. I. Son, and H. H. Bühlhoff, "Psychophysical evaluation of haptic feedback algorithms for the teleoperation of multi-uavs," in *International Conference on Ubiquitous Robots and Ambient Intelligence*, pp. 602–603, October 2010.
- [12] M.-D. Hua, T. Hamel, P. Morin, and C. Samson, "A control approach for thrust-propelled underactuated vehicles and its application to VTOL drones," *IEEE Transactions on Automatic Control*, vol. 54, pp. 1837–1853, August 2009.
- [13] D. Lee and K. Huang, "Passive-set-position-modulation framework for interactive robotic systems," *IEEE Transactions on Robotics*, vol. 26, no. 2, pp. 354–369, 2010.
- [14] G. Gescheider, *Psychophysics: the fundamentals*. L. Erlbaum Associates, 1997.
- [15] M. Wellner, A. Schaufelberger, J. v. Zitzewitz, and R. Riener, "Evaluation of visual and auditory feedback in virtual obstacle walking," *Presence: Teleoperators and Virtual Environments*, vol. 17, no. 5, pp. 512–524, 2008.
- [16] F. A. Wichmann and N. J. Hill, "The psychometric function: I. fitting, sampling and goodness-of-fit," *Perception and Psychophysics*, vol. 63, no. 8, pp. 1293–1313, 2001.
- [17] S. Stramigioli, R. Mahony, and P. Corke, "A novel approach to haptic tele-operation of aerial robot vehicles," in *Proceedings of IEEE International Conference on Robotics and Automation*, pp. 5302–5308, 2010.
- [18] H. I. Son, L. Chuang, A. Franchi, J. Kim, D. Lee, S.-W. Lee, H. H. Bühlhoff, and P. Robuffo Giordano, "Measuring an operator's maneuverability performance in the haptic teleoperation of multiple robots," in *IEEE/RSJ International Conference on Intelligent Robots and Systems*, September 2011, submitted.